JACS
JOURNAL OF THE AMERICAN CHEMICAL SOCIETY
Article
pubs.acs.org/JACS

Chiral Hierarchical Molecular Nanostructures on Two-Dimensional Surface by Controllable Trinary Self-Assembly

Jia Liu,[†] Ting Chen,[†] Xin Deng,[†] Dong Wang,*[,†] Jian Pei,[‡] and Li-Jun Wan*[,†]

[†]Institute of Chemistry, Chinese Academy of Sciences, Beijing 100190, China, and Beijing National Laboratory for Molecular Sciences, Beijing 100190, China

[‡]College of Chemistry and Molecular Engineering, Peking University, and Beijing National Laboratory for Molecular Sciences, Beijing 100190, China

Supporting Information

ABSTRACT: The bottom-up fabrication of surface hierarchical nanostructures is of great importance for the development of molecular nanostructures for chiral molecular recognition and enantioselective catalysis. Herein, we report the construction of a series of 2D chiral hierarchical structures by trinary molecular self-assembly with copper phthalocyanine (CuPc), 2,3,7,8,12,13-hexahexyloxy-truxenone (TrO23), and 1,3,5-tris(10-carboxydecyloxy) benzene (TCDB). A series of flower-like chiral hierarchical molecular architectures with increased generations are formed, and the details of these structures are investigated by high resolution scanning tunneling microscopy (STM). The flower-like hierarchical molecular architectures could be described by a unified configuration in which the lobe of each architecture is composed of a different number of triangular shape building units (TBUs). The off-axis edge-to-edge packing of TBUs confers the organizational chirality of the hierarchical assemblies. On the other hand, the TBUs can tile the surface in a vertex-sharing configuration, resulting in the expansion of chiral unit cells, which thereby further modulate the periodicity of chiral voids in the multilevel hierarchical assemblies. The formation of desired hierarchical structures could be controlled through tuning the molar ratio of each component in liquid phase. The results are significant for the design and fabrication of multicomponent chiral hierarchical molecular nanostructures.

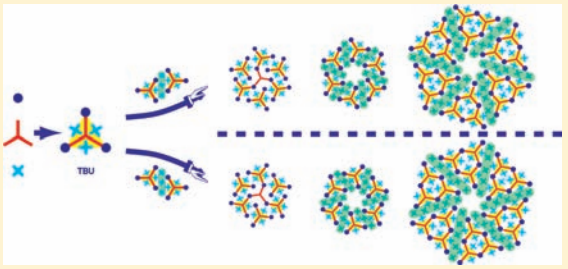

INTRODUCTION

Surface chirality has an intimate relationship with origin of chirality in nature, chiral molecular recognition, enantioselective catalysis, and many other important physical chemistry topics and has attracted great attention in recent years.[1−4] The spontaneous formation of enantiopure or racemic surface supramolecular patterns from the adsorption and assembly of chiral or pro-chiral molecules has been well-documented.[5−8] An intriguing phenomenon in surface chirality study is the formation of 2D organization chirality from nonchiral molecules, where the chirality is generated and steered by the arrangement of molecular building units in the 2D assemblies.[9−11] The underlying driving forces for the formation of chiral building units are typically the hydrogen bonding, dipole−dipole interaction, van der Waals interactions, and other weak interactions between functional groups. Understanding the formation of assembly building blocks, application and propagation of surface chirality in 2D supramolecular chiral assemblies is of ultimate importance to predict and control over the 2D supramolecular chirality. On the other hand, hierarchical self-assembly is ubiquitous in biological systems. Hierarchically formed architectures may exhibit excellent properties and functions that are not displayed by their individual components.[12−14] People have gained a lot of inspiration from biological systems for the design and fabrication of supramolecular functional systems.[15] Recently, scientists have made progress, and some two-dimensional multilevel hierarchical self-assembled architectures were fabricated by using organic molecular building blocks.[16−26] For example, trimesic acid can form a series of multilevel hierarchical self-assembly structures from "chicken wire" structure to different sizes of "flower" structures via the intermolecular hydrogen bonding.[27] Spillmann et al. reported the nanoporous two-dimensional supramolecular structures by the hierarchical assembly of organic molecules interconnected through metal−ligand coordination interaction.[28] The tripod-shaped bromo-adamantane trithiol (BATT) molecule was found to form two-tiered hierarchical chiral self-assembly on gold surface.[29] A hexaphenylbenzene (HPB) derivative was used to construct a hierarchical chiral honeycomb pattern.[30] Comparing with the relatively well-documented 2D architectures engineered from molecular tectons, the distinct feature of multilevel hierarchical molecular assemblies on surfaces is that the primary building unit is composed of molecular clusters interlinked via noncovalent interactions. Aside from the aesthetic-pleasing structures, the hierarchical assemblies typically display large and continuously tunable periodicity,

Received: October 11, 2011
Published: November 22, 2011

   dx.doi.org/10.1021/ja209469d | J. Am. Chem.Soc. 2011, 133, 21010−21015

high complexity, and variety and have broad application potential in nanopatterning, molecular electronics, and molecular devices.[31−33] The inherent complexity of hierarchical assemblies, on the other hand, imposes a great challenge to the detailed understanding of the underlying formation mechanism, which is of great importance to conceive and steer the assembly process to fabricate potential hierarchical molecular nanostructures. Therefore, it is still a challenge to fabricate multicomponent hierarchical molecular architecture with enhanced diversity and controllability.

Herein, we use 2,3,7,8,12,13-hexahexyloxy-truxenone (TrO23), 1,3,5-tris(10-carboxydecyloxy)benzene (TCDB), and copper phthalocyanine (CuPc) to fabricate a series of flower-like chiral hierarchical superstructures with the tunable periodicity in a size range from 7 nm to more than 14 nm on highly oriented pyrolytic graphite (HOPG). The chemical structures of TCDB, TrO23, and CuPc are shown in Scheme 1.

Scheme 1. (a) Molecular Structures of TCDB, TrO23, and CuPc and (b) Illustration of the Hierarchical Self-Assembly Formation Process

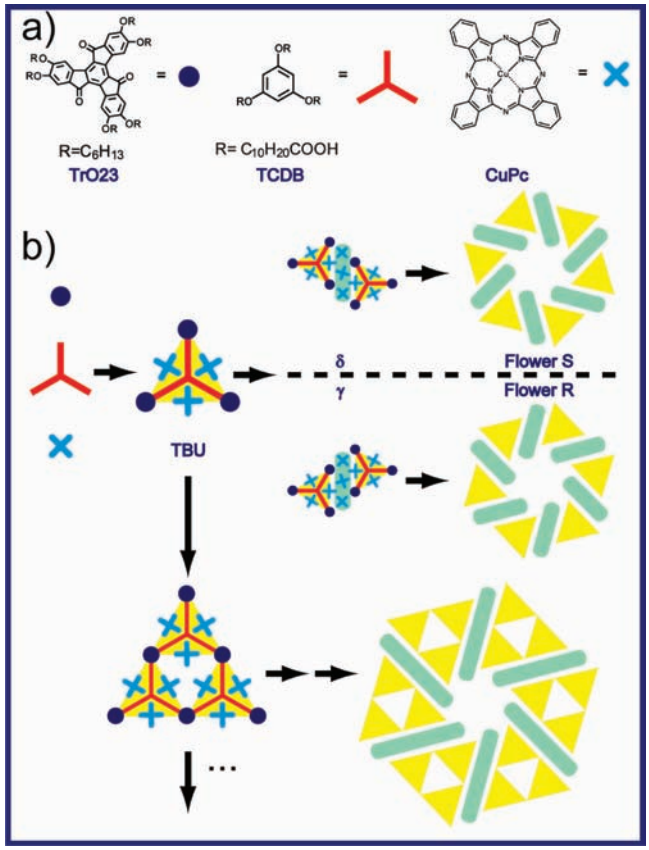

TCDB has three carboxyl terminated alkyl chains which can form a hydrogen bond with carbonyl groups of TrO23. The molecular structure of TrO23 is characterized by a flat truxenone aromatic core surrounded by six flexible hydrocarbon chains. Our previous result showed that TCDB and TrO23 can form a nanoporous network with the help of hydrogen bond and van der Waals interactions between them (Figure S1 in the Supporting Information, SI).[34] In this study, we have found that the participation of CuPc in the trinary assembly results in the formation of chiral superstructures. The assembling process of a typical hierarchical structure is schematically illustrated in Scheme 1b. A triangle shape building unit (TBU) composed of three TrO23, one TCDB, and three CuPc is the secondary building unit of the hierarchical assembly. Two TBUs can arrange in an edge-to-edge configuration by sharing a common CuPc lines as separator to form a rhombus unit cell. The main axes of two TBUs in a unit cell are offset slightly and form a prochiral hierarchical building unit, as denoted as δ and γ in Scheme 1b. The chirality of the building unit is further amplified by tiling the surface with these two chiral unit cells, resulting in the formation of a flower structure with chiral voids of 6-fold symmetry. Furthermore, the TBUs can tile the surface in a vertex-sharing configuration, resulting in the expansion of chiral unit cells, which thereby further modulate the periodicity of chiral voids in the multilevel hierarchical assemblies. The formation of specific multilevel hierarchical structures could be controlled through tuning the molar ratio of each component in the liquid phase. The tailored chiral hierarchical supramolecular assemblies on surfaces open up new possibilities for the bottom-up fabrication of complex functional nanostructures.

EXPERIMENTAL SECTION

TrO23 and TCDB were synthesized by the procedure reported in the literature.[40,41] CuPc was purchased from Aldrich and used without further purification. TrO23 was dissolved in 1-phenyloctane at concentrations from 5×10^{-5} to 10^{-7} M. CuPc was dissolved in 1-octanol to produce a saturated solution with a concentration about 10^{-6} M. TCDB was dissolved in 1-phenyloctane to make a saturated solution in a concentration about 1.5×10^{-5} M and diluted to the desired concentration before use. To prepare the trinary assemblies, a drop of CuPc saturated solution (ca. 4 μL) in 1-octanol was first deposited on HOPG, and the substrate was annealed to 100 °C (CuPc is stable at this temperature[42]) to remove the solvent; then a drop of the TrO23 solution (4 μL) and a drop of TCDB (4 μL) of desired concentration were applied onto the same HOPG surface successively. The adlayer structures were observed by using NanoScope IIIa (Veeco Inc. USA) STM with mechanically cut Pt/Ir (90/10) tips. All STM images presented here were recorded in a constant current mode and presented without further processing.

RESULTS AND DISCUSSION

Multilevel Hierarchical Assembly. The hierarchical assemblies are fabricated by successively deposition of CuPc, TCDB, and TrO23 on the HOPG surface. From the large scale STM image in Figure 1a, we can see a flower-like adlayer structure with an orderly distributed dark area enclosed by some bright spots. The structure is named **Flower 0**. The high resolution STM image in Figure 1b manifests more details. A unit cell is overlaid with the measured unit cell parameters of $a = b = 7.2 \pm 0.2$ nm, $\alpha = 60 \pm 2°$. In the dark holes of Flower 0, which are located at the corner of the unit cell, there are molecules with three chains extending to three bright spots. The angle between any two chains is about 120°, and the length of the chain is consistent with the alkyl chain length of TCDB. The molecules in the dark holes are therefore identified as TCDB molecules. Each unit cell contains two center-symmetrically arranged triangular clusters, as highlighted by the shaded triangle in Figure 1b. Each triangle consists of three sets of bright spots. The small spot illustrated by the dark blue circle has a diameter of about 1.0 ± 0.1 nm, consistent with the size of the truxenone core. The other set of spots with a diameter of about 1.6 nm appears in characteristic four lobes as illustrated by blue crosses, consistent with the chemical structure of CuPc.

dx.doi.org/10.1021/ja209469d | J. Am. Chem.Soc. 2011, 133, 21010–21015

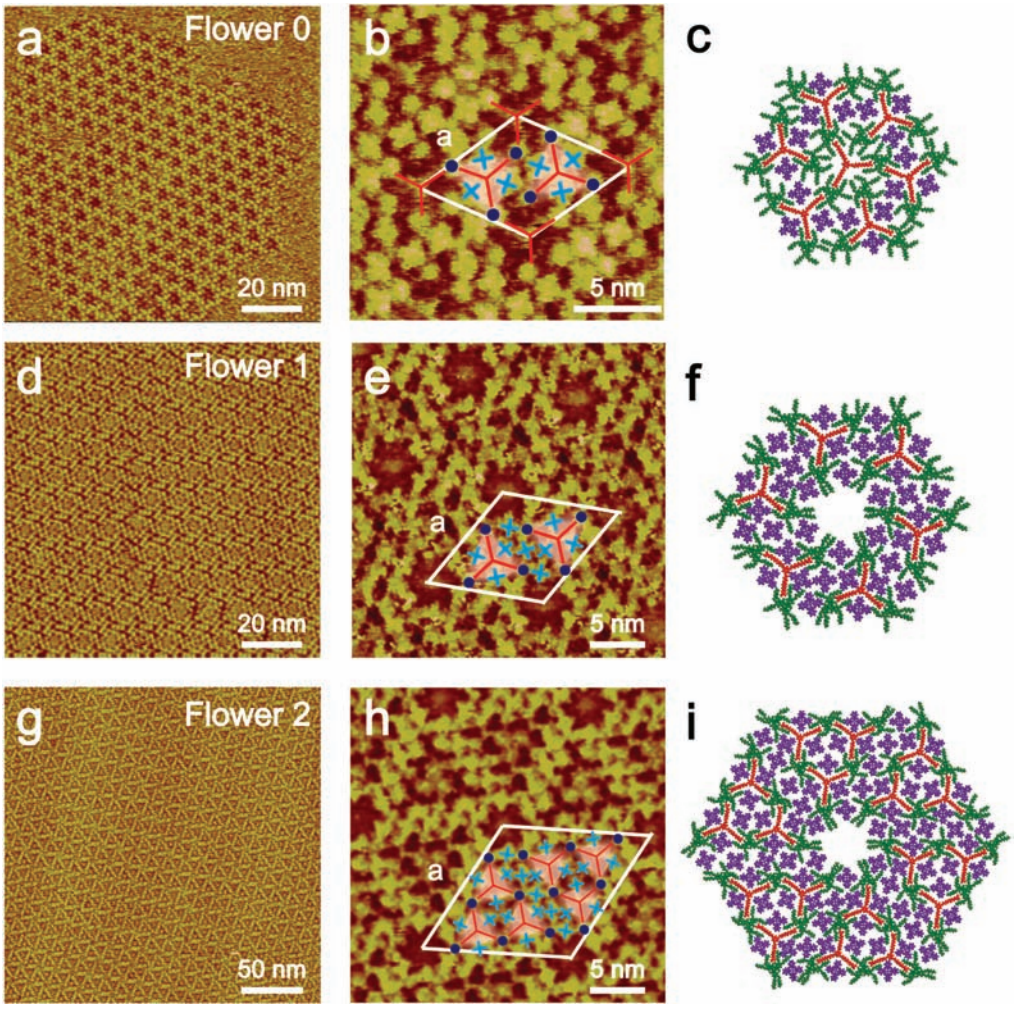

Figure 1. Multilevel hierarchical assembly. Large-scale (a,d,g) and high resolution (b,e,h) STM images of Flower 0 (a,b), Flower 1(d,e), and Flower 2 (g,h). Tunneling conditions: (a) I_{tip} = 366 pA, V_{bias} = 553 mV; (b) I_{tip} = 291 pA, V_{bias} = 463 mV; (d) I_{tip} = 473 pA, V_{bias} = 651 mV; (e) I_{tip} = 213 pA, V_{bias} = 633 mV; (g) I_{tip} = 365 pA, V_{bias} = 617 mV; (h) I_{tip} = 241 pA, V_{bias} = 430 mV. Structural models for Flower 0 (c), Flower 1 (f), and Flower 2 (i).

According to the diameter and appearance of large bright crosses, they can be attributed to CuPc molecules. A small bright spot is found at the centroid of the triangle. This spot is attributed to a TCDB molecule, which connects with TrO23 molecules at the corner of the triangle via hydrogen bonding between the terminal carboxylic acid group and the carbonyl group of TrO23.[34] The schematic symbols are overlaid in Figure 1b to illustrate the Flower 0 structure. On the basis of the above analysis, a structural model is presented in Figure 1c. The molecular ratio of TrO23, CuPc, and TCDB in Flower 0 is 2:2:1.

Figure 1d and g shows another two flower-like structures named as **Flower 1** and **Flower 2** obtained by tuning the concentration of TrO23 and TCDB in solution phase. The ordered adlayers with domain size larger than several hundred nanometers are obtained. The centers of Flower 1 or Flower 2 appear as "voids" in STM images, although some highly mobile molecules may adsorb in the center. The center "voids" of the two flowers have the same size and 6-fold symmetry. Careful inspection of the high resolution STM image of Flower 1 (Figure 1e) reveals similar triangular clusters as found in Flower 0. The triangle clusters are located at the center of the half-cell, as illustrated by the shaded triangles. Comparing with the Flower 0 structure, a noticeable feature is that there are three linearly arranged CuPc molecules between two neighboring triangles. Flower 2 shares many similar structural elements with Flower 1, except that the half cell is larger than Flower 1 and consists of three triangle clusters. Accordingly, the CuPc "separator" is composed of 5 CuPc molecules in Flower 2. The unit cell parameters of Flower 1 are $a = b = 9.2 \pm 0.2$ nm and $\alpha = 60 \pm 2°$, and those in Flower 2 are $a = b = 13.8 \pm 0.2$ nm and $\alpha = 60 \pm 2°$. The schematic models for Flower 1 and Flower 2 are superimposed in Figure 1e and h. Structure models for Flower 1 and Flower 2 are illustrated in Figure 1, parts f and i, respectively, and in good agreement with the STM images.

By tuning the molar ratio between three components, other flower-like structures with the same TBUs but different sizes are obtained (Figure S2). Figure 2 lists the structural details of the flower structures of different generations. For comparison, we outline each flower with one lobe superimposed with the schematic model and another with a green triangle. We can clearly see that all of the flowers' lobes contain the same TBUs as outlined by white triangles. Each TBU is composed of three CuPc, three TrO23, and one TCDB. The TBUs in these flowers represent primary supramolecular units with two distinct surface orientations, which can be correlated by a 60°

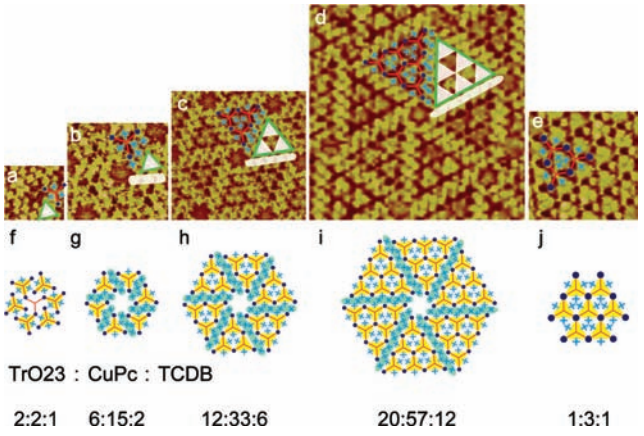

Figure 2. The structural evolution of hierarchical structures of different generations. (a)-(e) STM images of single flowers of Flowers 0, 1, 2, 3, and ∞. (f)-(j) schematic models for Flowers 0, 1, 2, 3, and ∞. Image sizes: (a) 11 × 11 nm^2; (b) 19 × 19 nm^2; (c) 25 × 25 nm^2; (d) 40 × 40 nm^2; (e) 20 × 20 nm^2. The relative molecular ratios between TrO23, CuPc, and TCDB in each self-assembled structures are shown below each STM image.

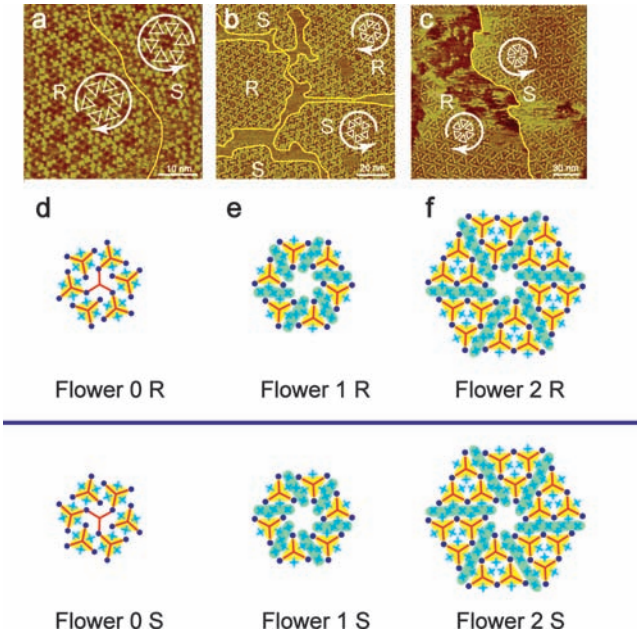

Figure 3. STM images show coexistence of enantiopure chiral structures of Flowers 0(a), 1(b), and 2(c). The imaging conditions are as follows: (a) I_{tip} = 213 pA, V_{bias} = 485 mV; (b) I_{tip} = 213 pA, V_{bias} = 633 mV; (c) I_{tip} = 241 pA, V_{bias} = 430 mV. (d-f) Strcutral models for chiral hierarchical assemblies.

rotation operation. All flower structures have six lobes. The lobe of Flower 0 is composed of one TBU. The TBUs in Flower 1 are divided by six separators composed of a CuPc triad as outlined in Figure 2b. There is no molecule in the center of Flower 1 and bigger flowers. Each lobe in Flower 2 is bigger than that of Flower 1 and composed of three TBUs. The three TBUs pack into a bigger triangular lobe by sharing vertexes, and neighboring lobes are separated by a CuPc separator, as outlined with a white bar in Figure 2c. Flower 2 can also be viewed as an expanded Flower 1 by addition of one more row of TBUs. Therefore, the generation of a flower is named by the number of TBU rows in its lobe, except Flower 0. Flower n ($n > 0$) are created by lobes with n rows of TBUs separated by CuPc separators with $2n+1$ CuPc molecules. Careful study reveals that CuPc molecules change their orientation alternately along the CuPc separators. The neighboring CuPc molecules in each flowers' CuPc separators have a crossing angle of 15° (Figure S3). A special case for the Flower n series is shown in Figure 2e, where the whole surface is covered by TBUs without the presence of a CuPc separator. This structure is named Flower ∞. Figure 2(f)-(j) shows schematic models for all the flower structures of different generations.

Chirality of Hierarchical Assembly. Owing to a spiral arrangement of flower lobes around the center voids, the trinary hierarchical assemblies show distinct surface organizational chirality. Panels a-c of Figure 3 show the coexistence of both enantiopure domains of Flowers 0, 1, and 2 in the same STM image. Both mirror-symmetric chiral domains of these flower-like architectures have been obtained. The numbers of the entiopure domains and the domain sizes are roughly equal, as expected. No defined correlation between the orientations of TBUs with the underlying HOPG substrate has been observed. Figure 3d-f shows the schematic models of chiral structures of Flowers 0, 1, and 2. The CuPc molecules along the edge of the TBUs and in the CuPc separators are offset from each other to avoid the steric crowding of CuPc molecules, following the Kitaigorodskii's principle of closest-packing.[35] As a result, the TBUs in each unit cell take an off-axis arrangement, which breaks down the mirror-symmetry of TBUs and confers organization chirality to the unit cell and the hierarchical assemblies. The chiral voids in the center of Flowers 1 and 2 and other high generation flower structures may act as a host template for enantioselective separation or chiral catalysis. Similar surface chirality of hierarchical assemblies has been observed in other one-component hierarchical assemblies.[17,32,33]

Structural Evolution of Hierarchical Structures. To understand the structural evolution of hierarchical structures of different generations, we calculated the molar ratio of three components in each flower structure, as presented at the bottom of Figure 2. The molecular ratio of TrO23, CuPc, and TCDB in Flower n can be deduced as $(n^2+3n+2):(3n^2+9n+3):(n^2+n)$ (See Figure S4 for the detailed deduction process.) for all the structures except Flower 0. The existence of TCDB in the flower center and the absence of CuPc separators make the molecular ratio in Flower 0 2:2:1 (6:6:3) and deviate from the tendency of the other structures. With the continuous increase of the flower lobes, the surface would be covered by the closely packed TBUs eventually, as presented in Figure 2e. The molecular ratio of TrO23, CuPc, and TCDB in Flower ∞ is 1:3:1, consistent with the result from the formula presented above.

The TrO23/CuPc/TCDB trinary assembly system consists of three components and is formed at solid−liquid interface. We found that the formation of the trinary hierarchical assemblies can be tuned by controlling the amount of individual components in the solution phase. Owing to the limited solubility of CuPc in phenyloctane, CuPc molecules are believed to adsorb preferentially on the surface and act as an excess component in the assembly. Therefore, we surveyed the self-assembled structures at varied amounts of TCDB and TrO23 in solution phase, while keeping the amount of CuPc constant. Figure 4a summarizes the results of the formation of different self-assembled structures by tuning the concentration

dx.doi.org/10.1021/ja209469d | J. Am. Chem.Soc. 2011, 133, 21010–21015

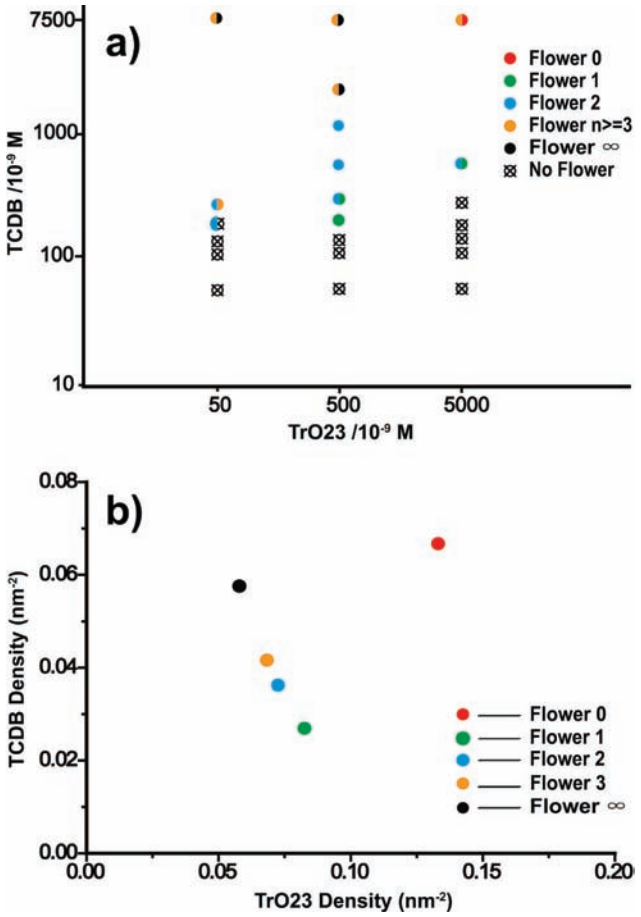

Figure 4. (a) Dependence of the observed hierarchical structures on the concentrations of TCDB and TrO23 in solution phase. The colors of the dots represent the hierarchical structures of different generations. (b) The surface coverage (density) of TCDB and TrO23 in hierarchical structures. The unit is molecule nm^{-2}.

of TCDB and TrO23 by keeping the solution volume constant. From Figure 4a we can learn that Flower 0 often appears when the concentration of TCDB and TrO23 are both high. Lowering the amount of TrO23 results in the formation of flower structures of higher generations. The flower structures of high generation are relatively more sensitive to the concentration change. The flower structure of low generations (1, 2) is favored when the concentration of TCDB and TrO23 are both at medium level. At properly tuned concentration, the pure phases of low generation flower structures can be obtained (i.e., Figure 1). Figure 4b plots the coverage of TCDB and TrO23 in flower structures of different generations. The correlation between Figure 4 parts a and b indicates that the formation of flower structures is controlled by the concentration of each component in the solution phase.

Similar multilevel hierarchical structures have been observed for the one-component self-assembly of other C_3 symmetry molecules such as TMA and a HPB derivative.[27,30] All these structures have six lobes, and each lobe contains C_3 symmetry components. In the case of TMA and HPB, the half-unit cells are bound to each other via dimeric hydrogen bonds, while the molecules within the half-unit cells are close-packed via weaker trimeric hydrogen bonds for TMA and van der Waals interactions for HPB. The formation of hierarchical structures of different generations is ascribed to the balance between intermolecular interactions (to drive the formation of porous structures) and molecular-substrate interactions (to drive the formation of close-packing structures).

In our system, each lobe of a flower structure is divided from each other by CuPc molecular separators, and the interactions at the boundary between each lobe are weak (van der Waals interaction). In contrast, the molecules within the lobe are relatively stronger via hydrogen bond combined with van der Waals interactions between CuPc, TCDB, and TrO23. One would expect the Flower ∞ is thermodynamically favored since the close-packed TBUs can simultaneously maximize the intermolecular interactions and molecular-substrate interactions. The observation of concentration-dependent multilevel hierarchical assemblies indicates that the solid/liquid interface plays an important role in the assembly process. The chemical potential of molecules in self-assembled nanostructures at the solid/liquid interface is at the dynamic equilibrium with that in the solution phase. The coverage of adsorbates on the surface is determined by the concentration of the molecules in the solution phase, although the dependence is typically nonlinear. Therefore, by tuning the concentration of TCDB and TrO23 in the solution phase, their coverage at the surface is tuned. TCDB, TrO23, and CuPc can form primary building block TBU through the hydrogen bonding and van der Waals interaction (Scheme 1). The TBU building blocks can further attach to each other to form lobes with different sizes in response to the molar ratio of TCDB and TrO23 at the surface. When CuPc is excess in the system, the formation of TBU building blocks is not able to deplete all the CuPc molecules. Since CuPc has limited solubility in phenyloctane, CuPc prefers to stay at the interface and organize itself into separators to the TBU lobes. In other words, the weak interaction between CuPc separators and TBU lobes is compensated by desolvation energy of CuPc at the solid/liquid interface. A similar solvent effect to modulate the self-assembly has been observed in other systems.[36−39] By increasing the concentration of TCDB in the solution phase, and thus the coverage of it on the surface, the lobes grow bigger and form hierarchical structures with higher generations. At high coverage and suitable molar ratio of TCDB and TrO23, Flower 0 is preferred since the center-sitting TCDB provides extra hydrogen bonding to stabilize the structure. Further theoretical modeling is underway to fully understand the assembly process in this system.

CONCLUSIONS

In summary, a series of flower-like chiral hierarchical superstructures are constructed on the HOPG surface by trinary self-assembly of TrO23, CuPc, and TCDB molecules. High resolution STM images reveal that the unified building block of these hierarchical structures is a TBU with one TCDB, three TrO23, and three CuPc. The off-axis arrangement of TBUs in neighboring lobes in each unit cell confers surface chirality of the resulted hierarchical assemblies. The TBUs can tile the surface in a vertex-sharing configuration, resulting in the expansion of chiral unit cells and thereby further modulating the periodicity of chiral voids in the multilevel hierarchical assemblies. The formation of hierarchical structures on the surface could be tailored by tuning the molar ratio of each component in the liquid phase. The results presented here are helpful to the rational design and fabrication of multicomponent functional chiral hierarchical molecular nanostructures.

■ ASSOCIATED CONTENT

Supporting Information

(1) STM image of the TCDB/TrO23 nanoporous network, (2) STM image of flowers bigger than Flower 2, (3) STM images and cartoon models of single flowers of Flowers 1 and 2, and (4) formulas to calculate the molecular ratio of TrO23, CuPc, and TCDB in each flower structure. This material is available free of charge via the Internet at http://pubs.acs.org.

■ AUTHOR INFORMATION

Corresponding Author

wangd@iccas.ac.cn; wanlijun@iccas.ac.cn

■ ACKNOWLEDGMENTS

The authors thank the financial supports from National Key Project on Basic Research (Grants 2011CB808700 and 2011CB932300), National Natural Science Foundation of China (Grants 20733004, 20821003, 20821120291, 91023013, 20905069, 21003131), and the Chinese Academy of Sciences.

■ REFERENCES

(1) Barlow, S. M.; Raval, R. *Surf. Sci. Rep.* **2003**, *50*, 201.
(2) Lorenzo, M. O.; Baddeley, C. J.; Muryn, C.; Raval, R. *Nature* **2000**, *404*, 376.
(3) Attard, G. A. *J. Phys. Chem. B* **2001**, *105*, 3158.
(4) Knudsen, M. M.; Kalashnyk, N.; Masini, F.; Cramer, J. R.; Laegsgaard, E.; Besenbacher, F.; Linderoth, T. R.; Gothelf, K. V. *J. Am. Chem. Soc.* **2011**, *133*, 4896.
(5) Fasel, R.; Parschau, M.; Ernst, K. H. *Nature* **2006**, *439*, 449.
(6) Chen, Q.; Richardson, N. V. *Nat. Mater.* **2003**, *2*, 324.
(7) Bohringer, M.; Morgenstern, K.; Schneider, W. D.; Berndt, R. *Angew. Chem., Int. Ed.* **1999**, *38*, 821.
(8) Weigelt, S.; Busse, C.; Petersen, L.; Rauls, E.; Hammer, B.; Gothelf, K. V.; Besenbacher, F.; Linderoth, T. R. *Nat. Mater.* **2006**, *5*, 112.
(9) Mercedes, C. C.; David, N. R. *Supramolecular Chirality*; Springer: Berlin, Heidelberg, New York, 2006.
(10) Teugels, L. G.; Avila-Bront, L. G.; Sibener, S. J. *J. Phys. Chem. C* **2011**, *115*, 2826.
(11) Elemans, J.; De Cat, I.; Xu, H.; De Feyter, S. *Chem. Soc. Rev.* **2009**, *38*, 722.
(12) Tirrell, M.; Kokkoli, E.; Biesalski, M. *Surf. Sci.* **2002**, *500*, 61.
(13) Elemans, J. A. A. W.; Rowan, A. E.; Nolte, R. J. M. *J. Mater. Chem.* **2003**, *13*, 2661.
(14) Newkome, G. R.; Wang, P.; Moorefield, C. N.; Cho, T. J.; Mohapatra, P. P.; Li, S.; Hwang, S.-H.; Lukoyanova, O.; Echegoyen, L.; Palagallo, J. A.; Iancu, V.; Hla, S.-W. *Science* **2006**, *312*, 1782.
(15) Sarikaya, M.; Tamerler, C.; Jen, A. K. Y.; Schulten, K.; Baneyx, F. *Nat. Mater.* **2003**, *2*, 577.
(16) Yokoyama, T.; Yokoyama, S.; Kamikado, T.; Okuno, Y.; Mashiko, S. *Nature* **2001**, *413*, 619.
(17) Écija, D.; Seufert, K.; Heim, D.; Auwärter, W.; Aurisicchio, C.; Fabbro, C.; Bonifazi, D.; Barth, J. V. *ACS Nano* **2010**, *4*, 4936.
(18) Guillermet, O.; Niemi, E.; Nagarajan, S.; Bouju, X.; Martrou, D.; Gourdon, A.; Gauthier, S. *Angew. Chem., Int. Ed.* **2009**, *48*, 1970.
(19) Bléger, D.; Kreher, D.; Mathevet, F.; Attias, A.-J.; Schull, G.; Huard, A.; Douillard, L.; Fiorini-Debuischert, C.; Charra, F. *Angew. Chem., Int. Ed.* **2007**, *46*, 7404.
(20) Blüm, M.-C.; Ćavar, E.; Pivetta, M.; Patthey, F.; Schneider, W.-D. *Angew. Chem., Int. Ed.* **2005**, *117*, 5468.
(21) Lei, S.; Surin, M.; Tahara, K.; Adisoejoso, J.; Lazzaroni, R.; Tobe, Y.; Feyter, S. D. *Nano Lett.* **2008**, *8*, 2541.
(22) Yang, Y.; Wang, C. *Chem. Soc. Rev.* **2009**, *38*, 2576.
(23) Huang, T.; Hu, Z.; Wang, B.; Chen, L.; Zhao, A.; Wang, H.; Hou, J. G. *J. Phys. Chem. B* **2007**, *111*, 6973.
(24) Wang, L.; Chen, Q.; Pan, G.-B.; Wan, L.-J.; Zhang, S.; Zhan, X.; Northrop, B. H.; Stang, P. J. *J. Am. Chem. Soc.* **2008**, *130*, 13433.
(25) Zhang, J.; Li, B.; Cui, X.; Wang, B.; Yang, J.; Hou, J. G. *J. Am. Chem. Soc.* **2009**, *131*, 5885.
(26) Canas-Ventura, M. E. C.-V. M. E.; Ait-Mansour, K.; Ruffieux, P.; Rieger, R.; Mullen, K.; Brune, H.; Fasel, R. *ACS Nano* **2011**, *5*, 457.
(27) Ye, Y.; Sun, W.; Wang, Y.; Shao, X.; Xu, X.; Cheng, F.; Li, J.; Wu, K. *J. Phys. Chem. C* **2007**, *111*, 10138.
(28) Spillmann, H.; Dmitriev, A.; Lin, N.; Messina, P.; Barth, J. V.; Kern, K. *J. Am. Chem. Soc.* **2003**, *125*, 10725.
(29) Katano, S.; Kim, Y.; Matsubara, H.; Kitagawa, T.; Kawai, M. *J. Am. Chem. Soc.* **2007**, *129*, 2511.
(30) Xiao, W.; Feng, X.; Ruffieux, P.; Gröning, O.; Müllen, K.; Fasel, R. *J. Am. Chem. Soc.* **2008**, *130*, 8910.
(31) Elser, V. *Phys. Rev. Lett.* **1989**, *62*, 2405.
(32) Pennec, Y.; Auwarter, W.; Schiffrin, A.; Weber-Bargioni, A.; Riemann, A.; Barth, J. V. *Nat. Nano* **2007**, *2*, 99.
(33) Lobo-Checa, J.; Matena, M.; Müller, K.; Dil, J. H.; Meier, F.; Gade, L. H.; Jung, T. A.; Stöhr, M. *Science* **2009**, *325*, 300.
(34) Liu, J.; Zhang, X.; Wang, D.; Wang, J.-Y.; Pei, J.; Peter, J., S.; Wan, L.-J. *Chem. Asian J.* **2011**, *6*, 2426.
(35) Kitaigorodskii, A. *Acta Crystallogr.* **1965**, *18*, 585.
(36) Liu, J.; Zhang, X.; Yan, H.-J.; Wang, D.; Wang, J.-Y.; Pei, J.; Wan, L.-J. *Langmuir* **2009**, *26*, 8195.
(37) Liu, J.; Wang, D.; Wang, J.-Y.; Pei, J.; Wan, L.-J. *Chem. Asian J.* **2011**, *6*, 424.
(38) Xu, H.; Minoia, A.; Tomović, Z. e.; Lazzaroni, R.; Meijer, E. W.; Schenning, A. P. H. J.; De Feyter, S. *ACS Nano* **2009**, *3*, 1016.
(39) Shao, X.; Luo, X.; Hu, X.; Wu, K. *J. Phys. Chem. B* **2005**, *110*, 1288.
(40) Wang, J.-Y.; Yan, J.; Li, Z.; Han, J.-M.; Ma, Y.; Bian, J.; Pei, J. *Chem.—Eur. J.* **2008**, *14*, 7760.
(41) Lu, J.; Zeng, Q.-d.; Wang, C.; Zheng, Q.-y.; Wan, L.; Bai, C. *J. Mater. Chem.* **2002**, *12*, 2856.
(42) Lawton, E. A. *J. Phys. Chem.* **1958**, *62*, 384.